

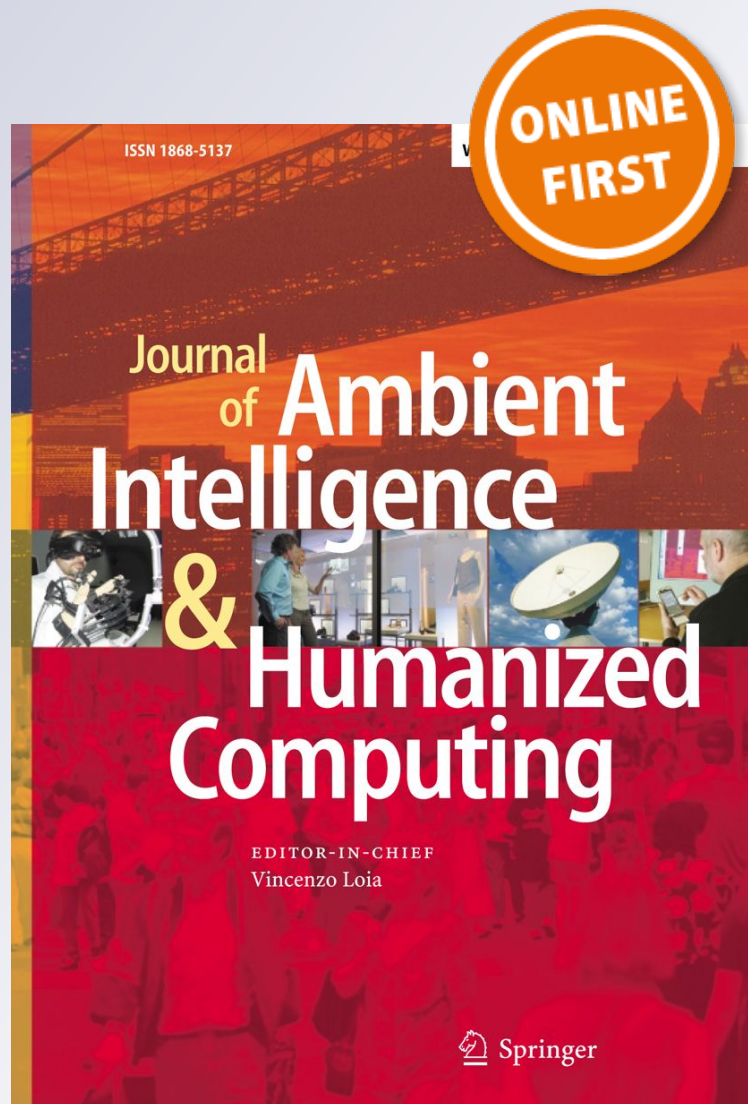
*Computer-based craniofacial  
superimposition in forensic identification  
using soft computing*

**B. Rosario Campomanes-Álvarez, Óscar  
Cordón, Sergio Damas & Óscar Ibáñez**

**Journal of Ambient Intelligence and  
Humanized Computing**

ISSN 1868-5137

J Ambient Intell Human Comput  
DOI 10.1007/s12652-012-0168-1



**Your article is protected by copyright and all rights are held exclusively by Springer-Verlag Berlin Heidelberg. This e-offprint is for personal use only and shall not be self-archived in electronic repositories. If you wish to self-archive your work, please use the accepted author's version for posting to your own website or your institution's repository. You may further deposit the accepted author's version on a funder's repository at a funder's request, provided it is not made publicly available until 12 months after publication.**

# Computer-based craniofacial superimposition in forensic identification using soft computing

B. Rosario Campomanes-Álvarez · Óscar Córdón · Sergio Damas · Óscar Ibáñez

Received: 22 June 2012 / Accepted: 8 October 2012  
© Springer-Verlag Berlin Heidelberg 2012

**Abstract** One of the most important tasks in forensic anthropology is human identification. Over the past decades, forensic anthropologists have focused on improving techniques to increase the accuracy of identification. Following a thorough examination of unidentified human remains, the investigator chooses a specific identification technique to be applied, depending on the availability of ante mortem and post mortem data. Craniofacial superimposition is a forensic process in which photographs of a missing person are compared with a skull in order to determine whether is the individual depicted and the skeletal remains are the same person. After more than one century of development, craniofacial superimposition has become an interdisciplinary research field where computer science has acquired a key role as a complement of forensic sciences. Moreover, the availability of new digital equipment has resulted in a significant advance in the applicability of this forensic identification technique. In this paper, we review a semi-automatic method devised to assist the forensic anthropologist in the identification process using craniofacial superimposition. The technique is based on a three-stage methodology. The first two are performed automatically by soft computing techniques. However, the

final decision corresponds to the forensic expert. The performance of the proposed method is illustrated using several real-world identification cases.

**Keywords** Forensic identification · Craniofacial superimposition · Skull 3D model reconstruction · Skull-face overlay · Evolutionary algorithms · Fuzzy landmarks

## 1 Introduction

Forensic anthropology studies medico-legal questions related to a deceased person through the examination of his skeletal remains (Burns 2007). The use of various identification techniques such as fingerprints, DNA profiles, or dental data comparison, depends mainly on the availability of information pertaining to a missing person and the condition of the remains to be compared, oftentimes, in missing persons cases, in mass graves or in mass fatalities, the available data is scanty (Iscan 1981). Hence, anthropological identification based only on skeletal information can be considered as the last resort for forensic identification. In this case, more specific skeleton-based identification techniques are alternatively implemented.

Among them, craniofacial superimposition (CS) is the most relevant technique (Krogman and Iscan 1986; Iscan 1993; Taylor and Brown 1998; Stephan 2009). This method aims to compare photographs of a “missing person” with a skull by superimposing photographs of the skull and of the missing person to establish whether they are same person by matching anthropological landmarks defined in the literature (Martin and Saller 1966).

These landmarks are located in two objects of different nature; the skull found, and the available face photograph

---

B. R. Campomanes-Álvarez (✉) · S. Damas · Ó. Ibáñez  
European Centre for Soft Computing,  
33600 Mieres, Asturias, Spain  
e-mail: rosario.campomanes@softcomputing.es

Ó. Córdón  
Department of Computer Science and Artificial Intelligence,  
University of Granada, 18014 Granada, Spain

Ó. Córdón  
Research Center on Information and Communication  
Technologies (CITIC-UGR), University of Granada,  
18014 Granada, Spain

resulting in a variant soft tissue depth among each pair of landmarks. In addition, their correspondence is not always symmetrical and perpendicular, some landmarks are located in a higher position in the living person and some others do not have a directly related landmark in the other set (George 1993; Iscan 1993). These facts, and the location of the landmarks, represent sources of uncertainty that should be tackled during the whole CS process. As a result, the final identification decision includes a certain degree of uncertainty (Yoshino et al. 1995; Jayaprakash et al. 2001).

Although CS has been in use for over a century, there is no systematic method but a trial and error approach is usually followed until a good superimposition is achieved. Considering that, “the orientation process is a very challenging and time-consuming part of the skull-photo superimposition technique and correctly adjusting the size and orienting the images can take several hours to complete” (Fenton et al. 2008), a systematic and automatic method for CS is a real need in forensic anthropology (Ubelaker 2000).

From the computer vision point of view, there is a clear relationship between the desired procedure and the image registration (IR) problem (Zitová and Flusser 2003). IR aims to find the transformation (rotation, translation, etc.) that overlays two or more pictures taken under different conditions, bringing the points as closely together as possible by minimizing the error of a given similarity metric.

CS can be tackled following an IR approach in order to overlay the skull over the face in the photograph but it involves a really complex optimization task. On the one hand, there is incomplete and vague information guiding the process while, on the other hand, the corresponding search space is vast and presents many local minima. Therefore, exhaustive search methods are not useful. Furthermore, forensic experts demand highly robust and accurate results. IR approaches based on evolutionary algorithms (EAs) are a promising solution for facing this challenging optimization problem (Bäck et al. 1997; Eiben and Smith 2003). Thanks to their global optimization nature, EAs own the capability to perform robust search in complex and ill-defined problems as IR (Damas et al. 2011a; Santamaría et al. 2010).

Forensic anthropologists usually express the identification decision according to several confidence levels, depending on the degree of conservation of the sample and of the analytical process put into effect: “absolute matching”, “absolute mismatching”, “relative matching”, “relative mismatching”, and “lack of information” (Jayaprakash et al. 2001; Yoshino et al. 1995).

During the last few years, a multidisciplinary team comprised by researches from the European Centre for Soft Computing and the University of Granada (Spain) has been working on this issue. They aim to propose a computer-based methodological framework to assist the forensic

anthropologist in human identification by means of the CS technique. The work focused on the design of an automatic method to reconstruct a 3D skull model from the original and to overlay it on a face photograph, exploiting the capabilities of soft computing (SC) in a two-fold manner (Bonissone 1997). EAs will be used to build a 3D model of the skull automatically and find the best fit between the skull found and the photograph of the face, while, fuzzy sets (FSs) will be considered in order to manage the different sources of uncertainty involved in the process (Zadeh 1965). In a final step, the forensic anthropologist will make an identification decision using the obtained superimposition.

The aim of this paper is to summarize this method including the latest developments and showing the results achieved over a real identification case. We first describe the most representative CS methods considered in the literature in Sect. 2. Section 3 is devoted to explain the proposal and the results obtained when solving a real-world case. Finally, Sect. 4 presents some conclusions and new open lines for future works.

## 2 Overview of craniofacial superimposition methods

The scientific basis of CS was established by Broca (1875) and Bertillon (1896) more than 100 years ago. Since then, CS evolved as new technology was available although its foundations were previously laid.

Martin and Saller (1966) proposed a series of anthropological measurements, indices, and features which are the base of anthropological studies nowadays. The first identifications by means of CS consisted of obtaining the negative of the original photograph of the face and marking the cephalometric landmarks on it. The same task was done with a photograph of the skull. Then, both negatives were overlapped and the positive was developed. This procedure was specifically named photographic superimposition (Glaister and Brash 1937).

Video superimposition has been preferred to photographic superimposition since the former is simpler and quicker. It overcomes the protracted time involved with photographic superimposition, where many photographs of the skull must be taken in varying orientations (Seta and Yoshino 1993).

The use of computers to assist forensic anthropologists in the identification process involved the next generation of CS systems (Pesce Delfino et al. 1986; Ubelaker et al. 1992). Beyond those works using computers just as storage devices or simple visualization tools, there are just a couple of proposals exploiting the real advantages of both digital devices and computer science, especially using computer graphics and artificial intelligence (Nickerson et al. 1991; Ghosh and Sinha 2001).

The process of superimposing the skull and the face images, requires (Chandra Sekharan 1993): (1) the determination of the real size of the figures i.e., scaling, and (2) orientation of the skull to correspond it with the position of the face in the photograph, using three possible movements: inclination, extension, and rotation.

In all the previous works, the overlay process relies on a number of corresponding anthropometrical landmarks proposed by Martin and Saller (1966) which has been used since then for the assessment of correspondence between the skull and the face (see Figs. 1, 2). The identification procedure can follow either an anatomical or an anthropometrical approach. The former relies on the morphology correlations between the skull and the face (Jayaprakash et al. 2001), while the latter, emphasizes the measurement of distances between pairs of landmarks and their comparisons to average facial tissue depths. It is also important to consider as many landmarks as possible, as well as different proportions among them (George 1993).

The variety of technological support for the CS technique from the initial identifications involved a large number of very diverse approaches found in the literature (Damas et al. 2011b).

### 3 Semi-automatic craniofacial superimposition using soft computing

The whole CS process is composed of three stages (Fig. 3), i.e. image acquiring, skull overlay, and decision making.

The first stage achieves a digital model of the skull and the enhancement of the image of the face. Obtaining an accurate 3D model of the skull has been considered a difficult task by forensic anthropologists in the past. However, this step can be easily achieved using advanced scanning devices like laser range scanners (Park et al. 2006). The subject of the identification process, i.e. the skull, is a 3D object. The use of a 3D model of the skull instead of a 2D image of the skull should be preferred as it is a more accurate representation. It has already been

shown that 3D models are much more informative in other forensic identification tasks (De Angelis et al. 2009). Concerning the image of the face, most recent systems use a 2D digital image. This stage also involves the application of image processing techniques to enhance the quality of the photograph of the face that was typically provided when the person disappeared (González and Woods 2008).

The second stage is the skull-face overlay (SFO) which consists of searching for the best overlay of both 2D images of the skull and face or of the 3D model of the skull and the 2D image of the face achieved during the first stage. A trial-error procedure looks for the best placement of the skull over the face considering the landmarks correspondences and the soft tissue depths at these points.

Finally, the third stage of the CS process corresponds to the decision making. Based on the SFO achieved, the identification decision is made by either judging the matching between the corresponding landmarks in the skull and in the face, or by analyzing the respective profiles. Also craniofacial morphanalysis is employed (Jayaprakash et al. 2001).

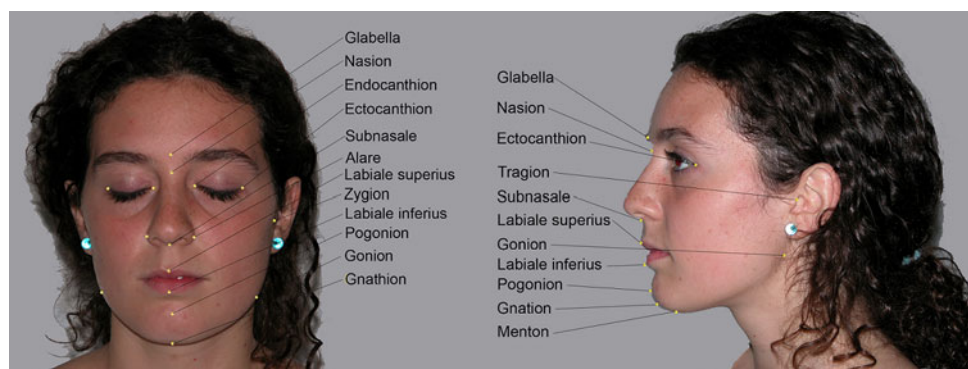
In order to automate the second stage and facilitate the first, we perform the former using a 3D model of the skull and a 2D digital image of the face. Then, we face the SFO stage as a 3D-2D IR problem, as will be explained below.

#### 3.1 First stage: 3D skull model reconstruction using EC

Since a whole object cannot be completely scanned in a single image using a range scanner, it is necessary to obtain and integrate multiple acquisitions from different views to construct the 3D model by a range image registration (RIR) algorithm (Dalley and Flynn 2001). This procedure is known as 3D model reconstruction and as a result a 3D model of the scanned object is obtained (Ikeuchi et al. 2001).

Some range scanners are equipped with a turn table device that is connected to the scanner and software for 3D reconstruction (Fig. 4) which require certain skills to deal with the set of 3D views usually by supervising the procedure of commercial software packages like RapidForm™, or when these software packages do not provide by

**Fig. 1** From left to right: principal facial landmarks, a lateral and b frontal views



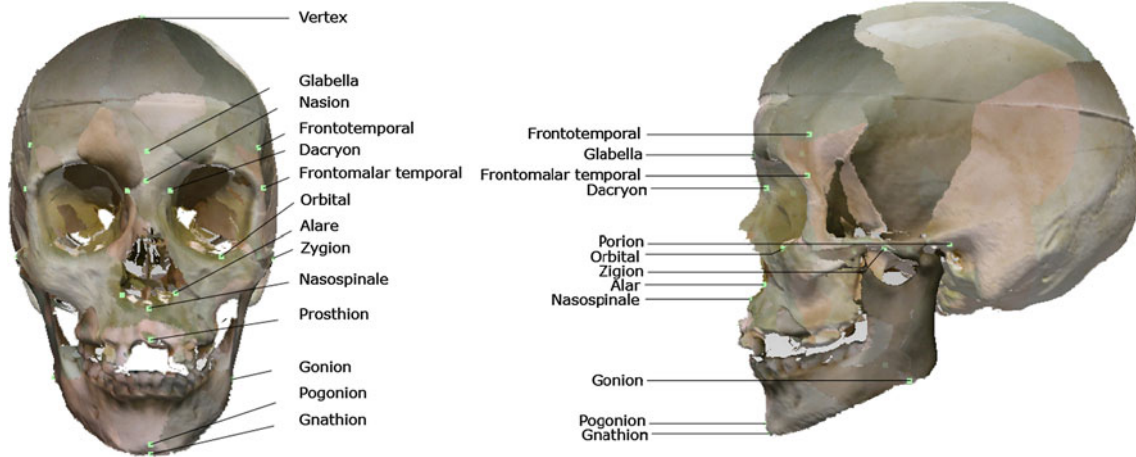
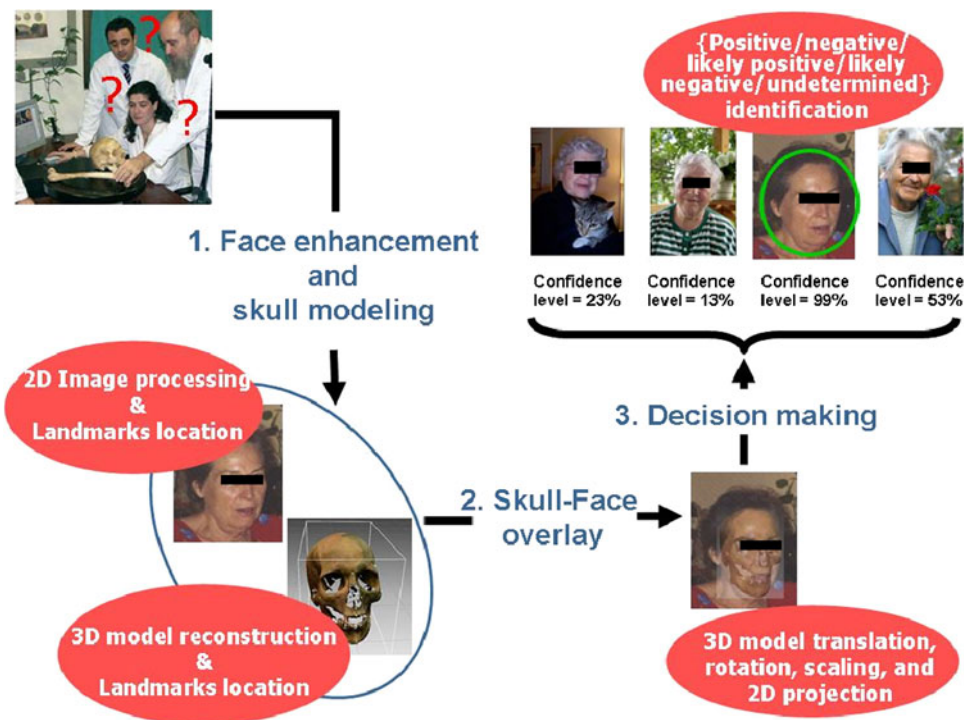


**Fig. 2** From *left to right*: principal craniometric landmarks, **a** lateral and **b** frontal views

**Fig. 3** The three stages involved in our proposed framework for the 3D/2D computer-aided CS process



“stitching up manually” every couple of adjacent views. In some instances the turn table is not available or is useless.

RIR using EC involves a complex optimization task, with a strongly multimodal and large search space. Thus, exhaustive search methods are not useful. A different approach was proposed by Santamaría et al. (2007a–c) which includes a pre-alignment stage that uses a scatter search (SS) (Laguna and Martí 2003) and a refinement stage based on the classical iterative closest point (ICP) algorithm (Besl and McKay 1992). The procedure is very robust because it reconstructs the 3D model of the skull even if the partial views of the skull present a very different orientation. (Santamaría et al. 2009a).

The proposed 3D reconstruction method carries out consecutive alignments of every pair of adjacent views, known as scene and model. The pair-wise RIR method aims to determine the Euclidean transformation that brings the *scene* view  $I_s = \{p_i\}_1^{N_{I_s}}$  into the best possible alignment with the *model* view  $I_m = \{q_i\}_1^{N_{I_m}}$ , where  $p_i$  and  $q_i$  are the points of the scene and the model, respectively. In particular, a 3D rigid transformation ( $f$ ) is determined by seven real-coded parameters, that is: a rotation  $R = (\theta, \text{Axis}_x, \text{Axis}_y, \text{Axis}_z)$  and a translation  $\vec{t} = (t_x, t_y, t_z)$ , with  $\theta$  and  $\text{Axis}$  being the angle and axis of rotation, respectively. Then, the transformed points of the *Scene* view are denoted by

$$f(p_i) = R(p_i - C_{I_s}) + C_{I_s} + t(p_i) = \{f(p_i)\}, \quad \forall i \in \{1, \dots, N_{I_s}\}, \quad (1)$$

where  $C_{I_s}$  is the center of mass of  $I_s$ .

In order to evaluate the accuracy of the estimated transformation the distance from a transformed  $I_s$  point  $f(p_i)$  to the *Model* view  $I_m$  is defined as the squared Euclidean distance to the closest point  $q_{cl}$  of  $I_m$ ,  $d_i^2 = \|f(p_i) - q_{cl}\|^2$ .

RIR can be formulated as an optimization problem that aims to determine the optimal Euclidean transformation  $f^*$  achieving the best overlapping of two images according to the considered *Similarity metric F*:

$$f^* = \arg \min_f F(I_s, I_m; f) \quad s.t. : f^*(I_s) \cong I_m \quad (2)$$



**Fig. 4** Acquisition of a skull 3D partial view by the use of the Konica-Minolta laser range scanner of the Physical Anthropology Laboratory at the University of Granada

The successful performance of any RIR method is drastically facilitated by the size of the common overlapping region present in two consecutive range images. However, a high overlapping ratio also increases drastically the number of skull views needed to acquire the whole 3D skull model. Hence, the authors considered those scanning cases with a minimum overlapping degree, close to the fifty percent of the physical surface, in order to ease the acquisition procedure to the forensic experts. Taking into account the said overlapping consideration, a robust objective function based on the minimization of the median squared error (*MedSE*) of the closest point distances  $d_i^2$  is considered:

$$F(I_s, I_m; f) = MedSE(d_i^2), \quad (3)$$

where  $MedSE()$  corresponds to the computation of the median  $d_i^2$  value of the  $N_{I_s}^{th}$  scene points. The authors used the grid closest point (GCP) scheme to speed up the closest point computation (Yamany et al. 1999).

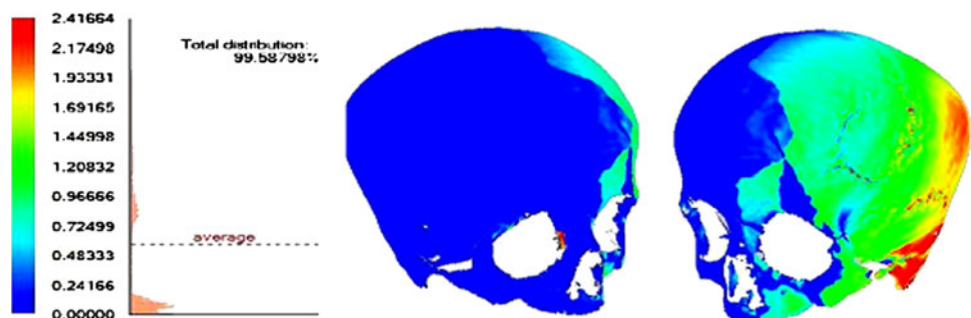
An example of a 3D skull model from the University of Granada Physical Anthropology Laboratory, automatically reconstructed from several partial views using the SS-based method proposed by Santamaría et al. (2009a), is shown in Fig. 5.

The forensic anthropologists established an average error allowed for the 3D skull model. Figure 6 depicts the distance deviation histogram comparing the reconstruction result and the ground-truth 3D model. The averaged error is less than 1 mm in most of the skull areas. An error higher than the average was observed only in the posterior area of the skull that is the least important for the cranio facial comparison.

**Fig. 5** From left to right: partial views of the skull



**Fig. 6** Distance deviation histogram comparing the reconstruction result and the ground-truth 3D model



### 3.2 Second stage: SFO by means of EAs and FSS

Searching for the best overlay of the 3D model of the skull achieved during the first stage, over the 2D digital image of the face, this process is guided by the correspondence between some anthropometrical landmarks on the skull (craniometric) and the face (cephalometric).

Formally, the SFO can be formulated as follows. Given two sets of 2D facial and 3D cranial landmarks  $F$  and  $C$ , respectively, both comprising  $N$  landmarks (Ibáñez et al. 2009a):

$$F = \begin{bmatrix} x_{f1} & y_{f1} & 1 & 1 \\ x_{f2} & y_{f2} & 1 & 1 \\ \dots & \dots & \dots & \dots \\ x_{fN} & y_{fN} & 1 & 1 \end{bmatrix}, C = \begin{bmatrix} x_{c1} & y_{c1} & z_{c1} & 1 \\ x_{c2} & y_{c2} & z_{c2} & 1 \\ \dots & \dots & \dots & \dots \\ x_{cN} & y_{cN} & z_{cN} & 1 \end{bmatrix}$$

The overlay procedure aims to solve the system of equations (Eq. 4) with the following twelve unknowns: a rotation represented by an axis ( $\mathbf{d}_x, \mathbf{d}_y, \mathbf{d}_z$ ) and angle  $\theta$ , a center of mass ( $\mathbf{r}_x, \mathbf{r}_y, \mathbf{r}_z$ ), a translation vector ( $\mathbf{t}_x, \mathbf{t}_y, \mathbf{t}_z$ ), a uniform scaling  $s$ , and a 3D–2D projection function that is given by a field of view  $\varphi$ . These twelve parameters determine the perspective transformation, which projects every cranial landmark  $c^i$  of the skull 3D model onto its corresponding facial landmark  $f^i$  of the photograph:

$$F = f(c) = C.(A.D_1.D_2.R_\theta.D_2^{-1}.D_1^{-1}.A^{-1}).S.T.P, \quad (4)$$

where  $\mathbf{R} = (A.D_1.D_2.R_\theta.D_2^{-1}.D_1^{-1}.A^{-1})$  represents a rotation matrix to orient the skull in the same pose of the photograph.  $S$ ,  $T$ , and  $P$  are uniform scaling, translation, and perspective projection matrices, respectively. The interested reader can refer to Hearn and Baker (1997) for a detailed description of the matrices in Eq. 4 and their relation with the twelve unknowns of the problem, as well as to Ibáñez et al. (2009a) for a deeper explanation.

Hence, SFO can be formulated as a 3D–2D IR problem that aims to match 3D craniometric and 2D cephalometric landmarks.

Different definitions of the fitness function were studied, and the one that achieved the best results was the mean error (ME):

$$ME = \frac{\sum_{i=1}^N \|f(c^i) - f^i\|}{N}, \quad (5)$$

where  $\|\cdot\|$  is the 2D Euclidean distance,  $N$  is the number of considered landmarks (provided by the forensic experts),  $c^i$  corresponds to every 3D craniometric landmark,  $f^i$  refers to every 2D facial landmark,  $f$  is the function that defines the geometric 3D-2D perspective transformation, and  $f(c^i)$  represents the projected skull 3D landmark  $c^i$  in the image/photograph plane. Notice also that this function is to be minimized.

In particular, Ibáñez et al. (2009a) proposed two different real-coded genetic algorithms depending on the crossover operator employed, the blend crossover (BLX- $\alpha$ ) (Eshelman 1993) and the simulated binary crossover (SBX) (Deb and Agrawal 1995). They also presented a multimodal genetic algorithm (GA) using the clearing procedure (Ibáñez et al. 2009b), a niching method that consists of sharing limited resources within subpopulations of individuals characterized by some similarities (Pérowski 1996).

Among these three GAs the one that achieved the best performance uses the SBX-crossover. However, it was slightly outperformed by another approach studied by Ibáñez et al. (2009a), based on the covariance matrix adaptation evolution strategy (CMA-ES) (Hansen and Ostermeier 2001). Using CMA-ES as optimizer involves a really good behavior while maintaining at least the same quality in the results.

Finally, a SS method (Laguna and Martí 2003) was recently proposed in Ibáñez et al. (2012a). In that work, the SS framework is considered in order to exploit problem specific information to achieve faster and more precise solutions. In particular, the rotation angles once the skull positioned in a frontal pose were delimited. Even though other evolutionary approaches have a really good behavior, achieving similar minima, this new proposal has been shown to converge faster than CMA-ES and to behave more robustly in view of the mean values obtained in the thirty runs developed.

The aforementioned approaches were able to model properly the 3D–2D IR problem, achieving a high performance for all the cases. However, they did not consider the different sources of uncertainty presented in the problem. Thus, the resulting overlays did not reach the level of quality required in many cases, depending on the pose of the face in the photograph and the number of landmarks the forensic expert was able to locate. To overcome these problems, Ibáñez et al. (2011) studied the different sources of uncertainty and proposed the use of fuzzy landmarks to overcome most of them. Ibáñez et al. (2011) distinguish between the uncertainty inherent to the objects under study and that associated with the overlay process (see Fig. 7).

They identified two inherent sources of uncertainty regarding the handled objects i.e., a skull and a face and their relationship. The *landmark location uncertainty* is related to the extremely difficult task to locate the points in an invariable place since the definition of any anthropometric landmark is imprecise in its own. *The landmark matching uncertainty* refers to the imprecision that is involved in the matching of two sets of landmarks corresponding to two different objects: a face and a skull (Fig. 8).

The other type of uncertainty is associated with the 3D skull-2D face overlay and it is not inherent to the object themselves but to the approach, as it tries to overlay a 3D

**Fig. 7** Scheme of differences between uncertainty inherent to the objects and that associated with the overlay process

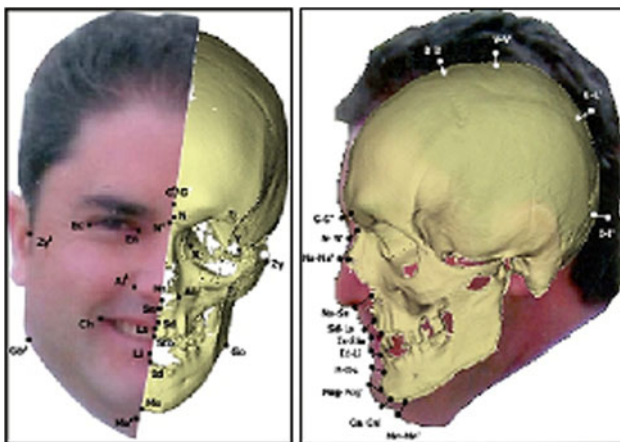
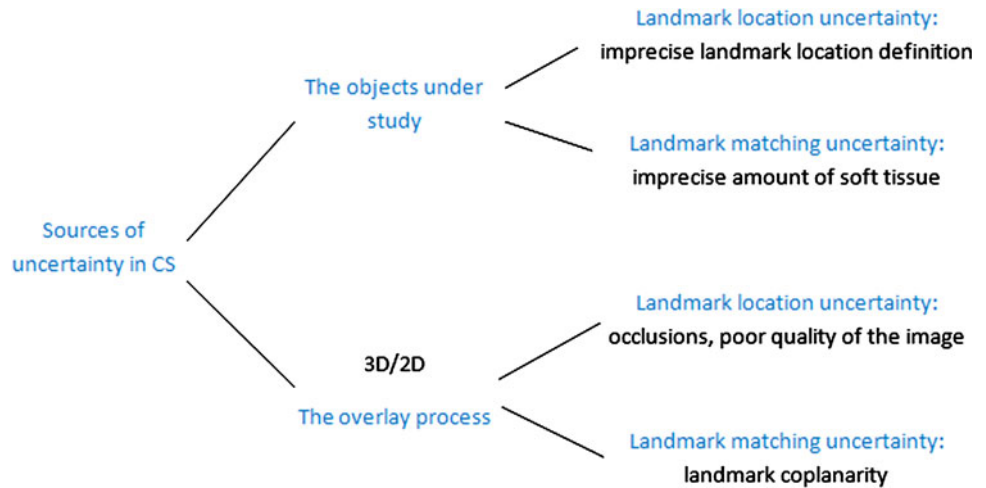


**Fig. 8** Correspondences between facial and craniometric landmarks: **a** lateral and **b** frontal views

model and a 2D image. Figure 9 shows examples of that situation.

The *landmark location uncertainty* refers to the difficulty to locate landmarks with the accuracy required for the automatic overlay of a 3D skull model and a 2D face photo, whereas the matching uncertainty refers to the negative influence of a small number of landmarks with an unsuitable spatial distribution in the quality of the SFO results as a consequence of the coplanarity problem (Santamaría et al. 2009b).

Two different approaches have been proposed to deal jointly with the imprecise landmark location and the coplanarity problem. Fuzzy landmarks allow the forensic experts to locate the cephalometric landmarks using ellipses and on considering FSs to model the uncertainty related to them. Besides, fuzzy distances are considered in order to model the distance between each pair of craniometric and cephalometric landmarks.

Following the idea of metric spaces in fuzzy landmark is defined as a fuzzy convex set of points having a nonempty

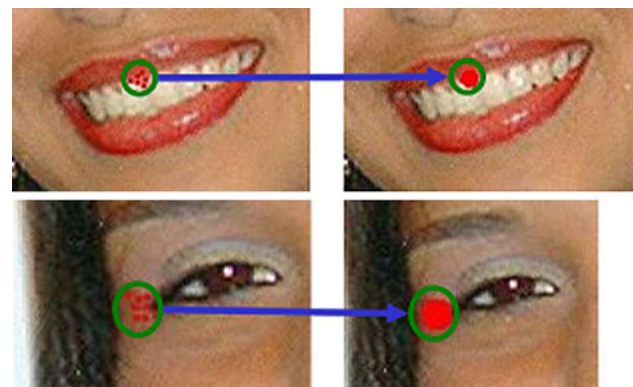


**Fig. 9** Examples of precise landmarks location by different forensic anthropologists. *Top row: a, b* Labiale superius landmarks. *Bottom row: a, b* right ectocanthion landmarks

core and a bounded support. All its  $\alpha$ -levels are nonempty bounded and convex sets (Diamond and Kloeden 2000).

Since the problem at hand deals with 2D photographs with and  $x \times y$  resolution, the fuzzy landmarks can be defined as 2D masks represented as a matrix  $m$  with  $m_x \times m_y$  points i.e., a discrete FSs of pixels. The size of each fuzzy landmark is different depending on the imprecision on its localization but at least one pixel (i.e. crisp point related to a matrix cell) will have membership with degree one.

An example of these fuzzy cephalometric landmarks is given in Fig. 10 on the left and the corresponding membership values of the pixels of one of those landmarks is depicted on the right.

The results of the present investigation indicate that a larger number of landmarks produce a more accurate overlay. The imprecise location of landmarks is a promising approach to avoid the coplanarity problem and to improve the performance of any SFO method, by allowing the anthropologist to locate additional landmarks that could not be otherwise determined.

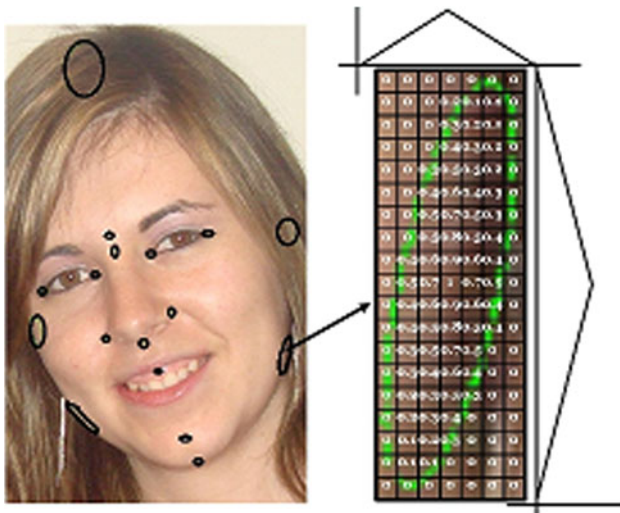


**Fig. 10** From left to right: **a** example of fuzzy location of cephalometric landmarks and **b** representation of an imprecise landmark using fuzzy sets

Based on nine complex real-world identification cases, the authors recognized that all the overlays achieved by their technique were competitive with the manual ones performed by the forensic experts. The proposed method successfully provided a good overall alignment of the skull and the face objects and achieved very accurate results and still behaved robustly.

Finally, a novel and alternative approach has been recently proposed by Ibáñez et al. (2012b) to deal with imprecise cephalometric landmarks in the SFO process. By using a cooperative co-evolutionary algorithm (CCEA), the authors were able to search for both the best transformation parameters and the best landmark location at the same time. Two different fitness functions were analyzed. One of them measured the mean distance between pairs of landmarks. The other weighted those distances by the corresponding value in a two-dimensional fuzzy set that models the imprecision in the location of each cephalometric landmark. Results are promising due to the very short time required by the co-evolutionary process. In fact, it is ten to forty times faster than the fuzzy-evolutionary methods and it yields high-quality overlays.

### 3.3 Application example: real-world cases solved using our automation approach

This section is devoted to illustrate the operation of the first two stages of the CS process that we have automated so far. To do so, we will first study the performance and the behavior of different methods that tackle the 3D reconstruction of a forensic object. Then, we will present the study of the performance of different EAs to model the imprecise location of cephalometric landmarks within our SFO method in comparison to a crisp location method.

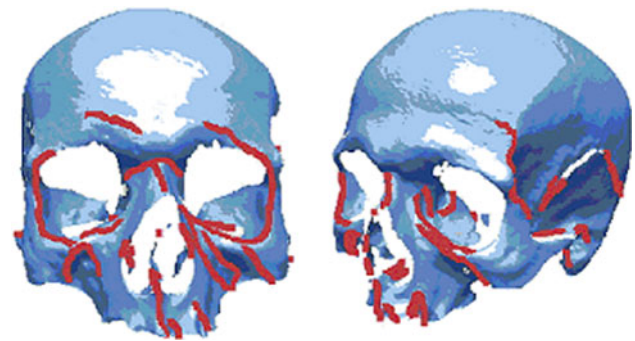


**Fig. 11** From left to right: **a** images  $I_{315^\circ}^1$  and  $I_{0^\circ}^1$ , each of the two images comprises both the original skull and **b** the crest line dataset

The forensic objects considered for this experimental study were chosen by the experts according to several forensic criteria. It is worth noting that the real-world case of the first stage does not correspond to the skull used in the second one.

#### 3.3.1 3D model acquisition and reconstruction

**3.3.1.1 Skull image datasets** The Physical Anthropology Laboratory of the University of Granada provided us with a human skull<sup>1</sup> acquired by a Konica-Minolta<sup>®</sup> 3D Lasser-scanner VI-910. We have taken into account important factors along the scanning process like time and storage demand. Following the suggestions in (Silva et al. 2005), we considered a scan every 45°. Hence, we deal with a sequence of eight different views: 0°–45°–90°–135°–180°–225°–270°–315°. The dataset we will use in our experiments is only limited to five of the eight views: 270°–315°–0°–45°–90°. Such a reduced subset of views is enough to perform a CS study as the obtained open 3D model includes all the required skull morphological characteristics.

We will consider a feature-based IR approach which aims to reduce the huge datasets IR algorithms typically deal with by selecting a small set of truly representative and invariant characteristics. We use a preprocessing algorithm that carries out the extraction of feature points from the range images (the skull views acquired by the laser scanner) by applying a 3D crest lines edge detector (Yoshizawa et al. 2005). Figure 11 shows some of the skull range images and their corresponding feature points.

Therefore, the resulting processed views will be used by every RIR method. Table 1 summarizes the size (number of image points) of the forensic range images of the considered skull before and after the application of the crest line extraction procedure.

<sup>1</sup> We cannot provide this dataset as public domain due to the Spanish law for protection of personal data.

**Table 1** Size of the range images of the considered dataset in their original conditions and after the feature extraction process

	Views/images				
	270°	315°	0°	45°	90°
Original	109,936	76,794	68,751	91,590	104,441
Crest lines	1,380	1,181	986	1,322	1,363

**3.3.1.2 Experimental design** We will focus our attention on the design of automatic, accurate, robust, and fast RIR methods based on memetic algorithms (MAs) (Krasnogor and Smith 2005), comparing their performance with those proposals existing in the IR literature adopting a sequential hybridization approach following the proposal in Santamaría et al. 2009a. The sequential hybridization between global and local strategies is becoming the current trend in the community (Dru et al. 2006; Jenkinson and Smith 2001; Yao and Goh 2006). In this sequential hybridization approach, a global search is first carried out taking advantage of the global search capability of EAs. Then, some kind of local search (LS) algorithm is used for fine tuning the result, usually as a separate stage. This scheme of hybridization is opposite to that considered by the memetic approach where the local search component is embedded in the global search procedure (Ishibuchi et al. 2003; Krasnogor and Smith 2005).

We have analyzed nine MAs resulting from the combination of three basic EAs: CHC (Eshelman 1991), differential evolution (DE) (Storn 1997), and scatter search (SS) (Glover 1977) and three LS techniques: Powell's (1964), Solis and Wets (1981), and crossover-based local search (XLS) (Beyer and Deb 2001) methods. The nine memetic designs will be compared to the three basic evolutionary approaches and to the nine sequential hybridizations resulting from their combination with the three selected local optimizers.

On the one hand, the experimental design addresses four different pair-wise RIR problems:  $I_{270^\circ}^1 - I_{315^\circ}^1$ ,  $I_{315^\circ}^1 - I_{0^\circ}^1$ ,  $I_{45^\circ}^1 - I_{0^\circ}^1$ . On the other hand, it is based on those ill-conditioned situations where forensics are advocated to manually intervene to reconstruct an optimal skull 3D model. That is the aim of the following RIR problem instances. They simulate an unsupervised scanning process where there is no turn table available or the particular environment does not allow its use. Specifically, the RIR instances are designed from a rigid transformation noted  $T_i$ , which is applied to one of the two images of every pair-wise RIR problem. For instance,  $T_i(I_{45^\circ}^2) - I_{0^\circ}^2$  represents a certain RIR instance to be tackled by every RIR method, where the rigid transformation  $T_i$  is applied to the  $I_{45^\circ}^2$  image to be placed in some other location different from its correct

original one. RIR methods aim to recover the original dataset location (the inverse transformation  $T_i^{-1}$ ) achieving a minimum distance (or maximum overlapping) criterion between the couple of images.

We will consider different rigid transformations  $T_i$  in every run of the considered RIR methods. Each of these transformations will simulate a typical bad situation for the forensics in which, for instance, there is no positional device or the object could suffer any displacement not being controlled by them. Indeed, such transformations (see Sect. 3.1) will be randomly generated with a uniform distribution as follows: each of the three rotation axis parameters will be in the range  $[-1, 1]$ ; the rotation angle will be in  $[0^\circ, 360^\circ]$ ; and the three translation parameters in  $[-40, 40]$ . This search space significantly influences (negatively, of course) the performance of classical RIR methods (Santamaría et al. 2007b; Zhang 1994), which usually deal with a transformation that slightly modifies the object location. Thus, any of the RIR methods considered in this work will have to overcome such really bad initializations to be considered an automatic, accurate, robust, and quick reconstruction method of forensic objects (skulls in the CS case).

**3.3.1.3 Parameter settings** The different RIR methods have been run on a 2.2 GHz. AMD ATHLON processor with 2 GB RAM and the GNU/Linux SuSe 10.1 (32 bits) O.S. using the GNU/gcc compiler without code optimization. Considering the speed requirement of our real-world application, both the MAs and the basic EA stage of the sequential hybridization approaches are run for the same fixed time of 20 s. In order to avoid execution dependence, every RIR method will tackle thirty different runs for each of the four considered RIR problem instances. Since we consider 20 s for the four sub problems comprising a skull reconstruction, we will be able to provide a skull open 3D model in just 80 s, which is a great improvement from the forensic expert point of view.

The three MA-based RIR methods (based on CHC, DE, and SS) are initialized with a population of 100 random solutions. The value of the parameter  $\alpha$  of the BLX- $\alpha$  operator employed in CHC is set to 0.5 (Cordón et al. 2006).

The best configuration we found for the control parameters of the DE-based MA is given by a mutation factor  $F = 0.5$  and a recombination rate  $CR = 0.7$ . In the SS-based MA, the reference set is composed of  $b = 8$  solutions and the BLX- $\alpha$  crossover operator is applied with  $\alpha = 0.3$  (Santamaría et al. 2007b).

The LS step of the sequential hybridization-based RIR methods (applied once the previous EA stage is finished) considers a stop criterion based on a predefined number of evaluations without improvement. In particular, we consider

**Table 2** Mean and standard deviation (in brackets) MedSE values for the three basic EAs, the nine sequential hybridization and MA-based RIR methods

Methods	Basic EAs	Sequential hybridizations			Memetic algorithms		
		Powell	Solis	XLS	Powell	Solis	XLS
CHC	30.75 (19.36)	30.20 (18.22)	30.98 (18.16)	30.17 (18.46)	30.84 (17.40)	30.75 (19.53)	28.91 (17.27)
DE	41.62 (19.74)	35.56 (18.29)	40.88 (18.47)	39.03 (18.22)	50.34 (20.49)	38.10 (20.04)	32.87 (19.33)
SS	31.45 (19.66)	31.38 (18.44)	31.45 (18.39)	31.45 (18.39)	36.80 (18.47)	26.81 (20.44)	<b>25.20 (17.66)</b>

Significant bold values treated as best result

4 *number-of-parameters-of-solutions* = 28. Notice that this final refinement step is not taken into account in the 20 s run time since it spends a very short amount of time. Even so, sequential hybridizations are slightly benefited from this consideration.

Finally, the restart mechanism is applied for DE and SS when the same population is kept during three iterations.

**3.3.1.4 Analysis of results** Table 2 presents the aggregated results of the basic EA, the sequential hybridization and the MA-based RIR methods.

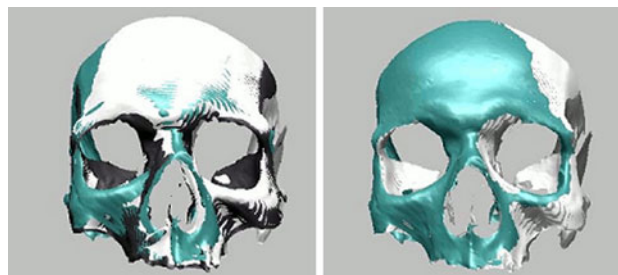
The best overall algorithm to tackle our 3D skull reconstruction task corresponds to a MA which considers SS as its EA and XLS method as its LS. It achieves the best performance with an averaged value of 25.20 against a 30.17, 35.56, and 31.38 for the best sequential hybridization based methods (*SH-CHC-XLS*, *SH-DE-Powell*, and *SH-SS-Powell*, respectively) as well as the other two best MA-based methods, *MA-CHC-XLS* and *MA-DE-XLS*, achieving values of 28.91 and 32.87, respectively.

Figure 12 shows the best reconstructed 3D model of the studied skull obtained by the MA-SS-XLS based RIR (on the left) and the perfect 3D model (on the right). In spite of the different colors that have been used to easily differentiate among the component 3D views, they perfectly overlap in the reconstructed model after the RIR process. Indeed, there is no visible difference between the reconstructed and the ground truth model in the skull.

### 3.3.2 3D–2D skull-face overlay

We have analyzed three different SFO problem instances corresponding to a real-world case previously addressed by the staff of the Physical Anthropology Laboratory in collaboration with the Spanish Scientific Police. The case of study happened in Cádiz, Spain. The three different photographs that are shown in Fig. 14 were provided by the relatives, who acquired them in different moments, poses, and conditions. Hence, this case study consists of three distinct SFO problem instances.

This identification case was positively solved following a computer-supported but manual approach for the SFO.



**Fig. 12** From left to right: **a** best reconstructed and **b** perfect model of the skull

We will consider the available 2D photographs of the missing person and the respective 3D skull model (Fig. 13) that was acquired using the Konica-Minolta 3D Laserscanner VI-910.

The forensic experts were able to locate 9, 11, and 12 landmarks following a crisp (precise) approach and 14, 16, and 15 using imprecise landmarks for poses 1, 2, and 3, respectively (see Fig. 14). These additional landmarks will play an essential role in order to tackle the coplanarity problem.<sup>2</sup> A clear example is the landmark on the top of the head, named *vertex*, which is never used by the forensic anthropologists because it is normally occluded by hair (and, thus, they are not able to precisely locate it), although it is very useful for the automatic overlay process since it lies in a complete different plane.

**3.3.2.1 Experimental design** We will study the performance of a real-coded genetic algorithm (RCGA) with the SBX crossover and the CMA-ES method, both presented in Ibáñez et al. (2009b). They include the fuzzy modeling of imprecise landmarks (Ibáñez et al. 2011). We named them f-RCGA and f-CMAES, respectively. In addition, we will also consider a cooperative co-evolutionary genetic algorithm (CCGA) proposed by Ibáñez et al. (2012a) to model the imprecise location of cephalometric landmarks within our SFO method. The latter uses a SBX crossover for the transformation parameters population and two-point

<sup>2</sup> Notice that these three images have a frontal or near-frontal pose of the face, and/or the corresponding craniometric set of landmarks is coplanar or near-coplanar.



**Fig. 13** Case study: 3D model of the skull

crossover for the landmark locations population. Random initial populations and random mutation are used in both cases, constraining the possible values for the landmark location to all the pixels inside the region corresponding to the imprecise landmark the forensic expert located in the image.

The set of employed parameters are the same described in Ibáñez et al. (2012b).

We would like to have a quantitative and objective measure to benchmark the achieved outcomes. Unfortunately, the ME values obtained by each approach are not fully significant to perform a comparison because of the different objective functions to be minimized. In addition, there is no a direct correspondence between ME values and the visual representations as was pointed out by the experts from the Physical Anthropology Laboratory at the University of Granada (Spain) in Ibáñez et al. (2011).

Due to the latter reasons, we adopted an alternative, specifically designed image-processing scheme, called area deviation error (ADE) (Ibáñez et al. 2011). It is based on evaluating the quality of the overlay by measuring the proper adjustment of the projected skull and the original face contours.

Despite some shortcomings, the ADE successfully provides a fair numerical index to compare the obtained SFO in an objective way, which properly complements the qualitative forensic anthropologist' assessment (Ibáñez et al. 2011).

**3.3.2.2 Analysis of results** Table 3 shows the run time (in seconds) needed by all the approaches in each of the SFO instances.

According to run time, the co-evolutionary approach achieves the best run time results for each pose. Indeed, the use of FSs in CCGA does not imply an increment in the run



**Fig. 14** Case study (left to right): photographs of the missing person corresponding to poses 1, 2, and 3. Pictures in the top row show the used crisp landmarks sets, which are composed of 9, 11, and 12 crisp landmarks, respectively. Pictures in the bottom row show the used imprecise landmarks sets, which are composed of 14, 16 and, 15 landmarks, respectively

**Table 3** Run time (seconds) needed to perform the fuzzy-evolutionary, the co-evolutionary and the crisp-evolutionary approaches over each of the SFO instances

Approach	Run time		
	Pose 1	Pose 2	Pose 3
CMA-ES	24"	23"	61"
f-CMAES	12"	13"	10"
f-RCGA	47"	73"	146"
CCGA	<b>4"</b>	<b>4"</b>	<b>4"</b>

Significant bold values treated as best result

time since CCGA avoids the calculation of fuzzy distances. Moreover, it is significantly faster than f-CMAES and f-RCGA, and at least, two times faster than the crisp CMA-ES approach. The comparison between the two fuzzy algorithms shows that the run time of f-CMAES is twice the f-RCGA time, so that latter approach clearly outperforms f-CMAES.

Table 4 presents the ADE values for the obtained overlays in the three instances (poses) of the considered case. Fuzzy-evolutionary (f-CMAES, f-RCGA), co-evolutionary (CCGA), and a crisp evolutionary (CMA-ES) approach are distinguished. The minimum (*m*), maximum (*M*), mean ( $\varpi$ ), and standard deviation ( $\sigma$ ) ADE values of the 30 runs performed are shown for each pose.

Following the results of Table 4, it can be seen that the worst behavior corresponds to the crisp approach. CMA-ES achieves worse results than the rest of the tested methods.

Figures 15, 16, 17 and 18 show the best superimposition for the three poses obtained using CMA-ES, f-CMA-ES, f-RCGA and CCGA, respectively.

Figure 15a presents the superimposition achieved by CMA-ES in the first pose. The skull does not coincide with the face of the photograph. f-CMAES (Fig. 16a), f-RCGA

**Table 4** Area-deviation-error (ADE) values in the best SFO estimations for each approach

Instance	Approach	ADE			
		$m$	$M$	$\varpi$	$\sigma$
1	CMA-ES	49.820827	52.994709	51.1051702	0.70216713
	f-CMAES	28.792446	30.720665	29.5870543	<b>0.45327576</b>
	f-RCGA	20.266197	<b>29.298676</b>	25.0512862	2.46768166
	CCGA	<b>20.101246</b>	30.709288	<b>24.913448</b>	2.7747241
2	CMA-ES	43.248581	46.787495	45.58037	0.7342788
	f-CMAES	20.85522	<b>22.272806</b>	21.63374	<b>0.4321111</b>
	f-RCGA	19.214912	28.268339	22.464926	2.0538164
	CCGA	<b>18.330183</b>	23.664318	<b>21.026742</b>	1.335274
3	CMA-ES	49.925446	55.599442	53.380075	1.6042135
	f-CMAES	17.90711	25.161003	18.81185	<b>1.2528082</b>
	f-RCGA	15.446845	25.640049	18.459968	2.3442206
	CCGA	<b>14.181023</b>	<b>20.075504</b>	<b>16.460508</b>	1.4287478

Significant bold values treated as best result



**Fig. 15** Best superimposition obtained using CMA-ES. **a** Pose 1, **b** pose 2, and **c** pose 3



**Fig. 17** Best superimposition obtained using f-RCGA. **a** Pose 1, **b** pose 2, and **c** pose 3

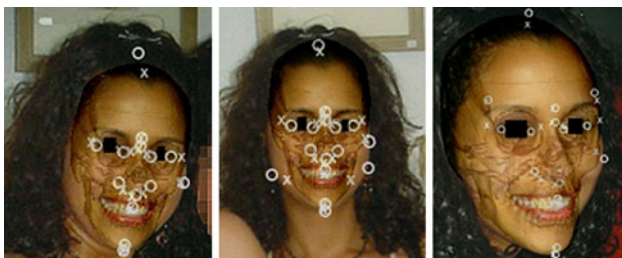


**Fig. 16** Best superimposition obtained using f-CMAES. **a** Pose 1, **b** pose 2, and **c** pose 3

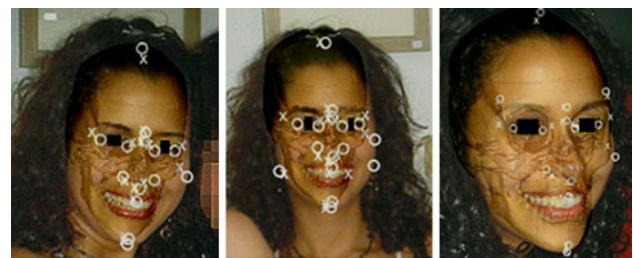


**Fig. 18** Best superimposition obtained using CCGA. **a** Pose 1, **b** pose 2, and **c** pose 3

(Fig. 17a), and CCGA (Fig. 18a) obtained more precise SFO results than CMA-ES (Fig. 15a) for the first instance.

Regarding the second pose, CMA-ES achieves a smaller skull area over the face of the photograph (Fig. 15b) than the remaining algorithms. Figure 15c shows the superimposition results for CMA-ES in the third instance. The right bottom area of the skull does not properly fit to the face of the photograph.

A direct comparison between f-CMAES and f-RCGA ADE values show they perform robustly (mean values),

achieving similar results. According to the mean values, f-RCGA is better than f-CMAES in the first instance (29.29 against 30.72). Meanwhile, the latter approach obtains a lower mean value in the second pose (22.27 vs. 28.26). Finally, they achieve very similar values in the third instance, 25.16 for f-CMAES and 25.64 for f-RCGA.

On the other hand, f-RCGA outperforms f-CMAES in the three instances with respect to the minimum values.

Figures 16 and 17 present the best superimposition results obtained by f-CMAES and f-RCGA,

respectively. f-RCGA achieves a more accurate SFO than f-CMAES for the first and second instances. Figure 17a, b show that f-RCGA obtains a lower distance between the landmarks of the skull and the face than f-CMAES (Fig. 16a, b).

Finally, f-RCGA and f-CMAES results are very similar for the third pose (Figs. 17c, 16c). There is almost no visual difference between the latter algorithms.

#### 4 Concluding remarks and future works

The aim of the present work was to design a complete, automatic, soft computing-based procedure to aid the forensic anthropologist in the identification task using CS. An semi-automatic method based on the use of real-coded EAs and FSs for solving the first two stages of the CS process: 3D skull model reconstruction and SFO was reviewed.

Such methods are fast, and robust, making them useful in solving a tedious task using a systematic approach although the technique still requires some improvements, it could be used as a tangible tool for obtaining a good superimposition automatically. Such a preliminary solution would be then manually refined by the forensic expert in a quick way.

The innovate technique we have reviewed in this paper is the result of several projects (SOCOVIFI TIN2006-00829 and the current SIMMRA TIN2009-07727) where we have performed an automatic procedure to support forensic anthropologists in the CS process.

This approach can be considered the most advanced semi-automatic system in the field, the Physical Anthropology Laboratory at the University of Granada has used the technique to solve several identification real-world cases for the Spanish Police.

In addition, the system (PCT/ES2010/00350) commercialized in Mexico, has received the IFSA Award for Outstanding Applications of Fuzzy Technology (2011) and the EUSFLAT Best Ph.D. Thesis Award (2011).

In the future, once the method has been thoroughly tested, the results should be validated through a more extensive study.

The inherent matching uncertainty regarding each pair of cephalometric-craniometric landmarks, should be addressed (Stephan and Simpson 2008a, b), as well as partial matching situation by means of FSs and fuzzy distance measures.

**Acknowledgments** This work has been supported by the Spanish Ministerio de Educación y Ciencia under the project TIN2009-07727. The authors would like to thank the team of the Physical

Anthropology Laboratory of the University of Granada for providing us with real-world cases for our analysis.

#### References

- Bäck T, Fogel DB, Michalewicz Z (1997) Handbook of Evolutionary Computation. IOP Publishing Ltd and Oxford University Press, Bristol
- Bertillon A (1896) Signaletic instructions: including the theory and practice of anthropometrical identification. The Werner Company, Chicago
- Besl PJ, McKay ND (1992) A method for registration of 3-D shapes. IEEE Trans on Pattern Anal and Mach Intell 14:239–256
- Beyer HG, Deb K (2001) On self-adaptive features in real-parameter evolutionary algorithms. IEEE Trans Evol Comput 5:250–270
- Bonissone P (1997) Soft computing: the convergence of emerging reasoning technologies. Soft Comput 1:6–18
- Broca P (1875) Instructions craniologiques et craniométriques de la Société d'Anthropologie de Paris. In: Mason G (ed) Paris, pp 63–96
- Burns K (2007) Forensic anthropology training manual. Pearson/Prentice-Hall, Utah
- Chandra Sekharan P (1993) Positioning the skull for superimposition. In: Iscan MY, Helmer R (eds) Forensic analysis of the skull. Wiley-Liss, New York, pp 105–118
- Cordón O, Damas S, Santamaría J (2006) Feature-based image registration by means of the CHC evolutionary algorithm. Image Vis Comput 22:525–533
- Dalley G, Flynn P (2001) Range image registration: a software platform and empirical evaluation. In: Third international conference on 3-D digital imaging and modeling (3DIM'01), pp 246–253
- Damas S, Cordón O, Santamaría J (2011a) Medical image registration using evolutionary computation: an experimental survey. IEEE Comput Intell Mag 6(4):26–42
- Damas S, Cordón O, Ibáñez O, Santamaría J, Alemán I, Navarro F, Botella M (2011b) Forensic identification by computer-aided craniofacial superimposition: a survey. ACM Comput Surv 43(4):1–27
- De Angelis D, Sala R, Cantatore A, Grandi M, Cattaneo C (2009) A new computer-assisted technique to aid personal identification. Int J Leg Med 123(4):351–356
- Deb K, Agrawal RB (1995) Simulated binary crossover for continuous search space. Complex Syst 9:115–148
- Diamond P, Kloeden P (2000) Metric topology of fuzzy numbers and fuzzy analysis. In: Dubois D, Prade H (eds) Fundamentals of fuzzy sets. Kluwer, Boston, pp 583–637
- Dru F, Wachowiak MP, Peters TM (2006) An ITK framework for deterministic global optimization for medical image registration. Proc SPIE Med Imaging Image Process 6144:1–12
- Eiben A, Smith J (2003) Introduction to evolutionary computing (natural computing series). Springer, Berlin
- Eshelman LJ (1991) The CHC adaptive search algorithm: how to safe search when engaging in nontraditional genetic recombination. In: Rawlins GJE (ed) Foundations of genetic algorithms 1. Morgan Kaufmann, San Mateo, pp 265–283
- Eshelman LJ (1993) Real-coded genetic algorithms and interval schemata. In: Whitley LD (ed) Foundations of genetic algorithms 2. Morgan Kaufmann, San Mateo, pp 187–202
- Fenton TW, Heard AN, Sauer NJ (2008) Skull-photo superimposition and border deaths: identification through exclusion and the failure to exclude. J Foren Sci 53(1):34–40

- George RM (1993) Anatomical and artistic guidelines for forensic facial reconstruction. In: Iscan MY, Helmer R (eds) *Forensic analysis of the skull* 16. Wiley-Liss, New York, pp 215–227
- Ghosh A, Sinha P (2001) An economised craniofacial identification system. *J Foren Sci Int* 117(1–2):109–119
- Glaister J, Brash J (1937) *Medico-legal aspects of the Ruxton case*. E & S Livingstone, Edinburgh
- Glover F (1977) Heuristic for integer programming using surrogate constraints. *J Decis Sci* 8:156–166
- González RC, Woods RE (2008) *Digital image processing*. Pearson Prentice, Upper Saddle River
- Hansen N, Ostermeier A (2001) Completely derandomized self-adaptation in evolution strategies. *Evol Comp* 9(2):159–195
- Hearn D, Baker MP (1997) *Computer graphics: C version*. Prentice Hall, Upper Saddle River
- Ibáñez O, Ballerini L, Córdón O, Damas S, Santamaría J (2009a) An experimental study on the applicability of evolutionary algorithms to craniofacial superimposition in forensic identification. *Inf Sci* 179(23):3998–4028
- Ibáñez O, Córdón O, Damas S, Santamaría J (2009b) Multimodal genetic algorithms for craniofacial superimposition. In: Raymond C (ed) *Nature-inspired informatics for intelligent applications and knowledge discovery: implications in business, science and engineering*, pp 119–142
- Ibáñez O, Córdón O, Damas S, Santamaría J (2011) Modeling the skull-face overlay uncertainty using fuzzy sets. *IEEE Trans Fuzzy Syst* 19(5):946–959
- Ibáñez O, Córdón O, Damas S, Santamaría J (2012a) An advanced scatter search design for skull-face overlay in craniofacial superimposition. *Experts Syst Appl* 39(1):1459–1473
- Ibáñez O, Córdón O, Damas S (2012b) A cooperative coevolutionary approach dealing with the skull-face overlay uncertainty in forensic identification by craniofacial superimposition. *Soft Comput* 16(5):797–808
- Ikeuchi K, Sato Y, Nishino K, Sato I (2001) Modeling from reality: photometric aspect. *Trans Virtual Real Soc Jpn* 4(4):623–630
- Iscan M (1981) *Integral forensic anthropology*. *Pract Anthropol* 3(4):21–30
- Iscan MY (1993) Introduction to techniques for photographic comparison. In: Iscan MY, Helmer R (eds) *Forensic analysis of the skull*. Wiley, New York, pp 57–90
- Ishibuchi H, Yoshida T, Murata T (2003) Balance between genetic search and local search in memetic algorithms for multiobjective permutation flow shop scheduling. *IEEE Trans Evol Comp* 7(2):204–223
- Jayaprakash PT, Srinivasan GJ, Amraveswaran MG (2001) Craniofacial morphoanalysis: a new method for enhancing reliability while identifying skulls by photosuperimposition. *Foren Sci Int* 117:121–143
- Jenkinson M, Smith S (2001) A global optimisation method for robust affine registration of brain images. *Med Image Anal* 5(2):143–156
- Krasnogor N, Smith J (2005) A tutorial for competent memetic algorithms: model, taxonomy and design issues. *IEEE Trans Evol Comp* 9(5):474–488
- Krogman WM, Iscan MY (1986) *The human skeleton in forensic medicine*, 2nd edn. Charles C. Thomas, Springfield
- Laguna M, Martí R (2003) *Scatter search: methodology and implementations*. Kluwer Academic Publishers, Boston
- Martin R, Saller K (1966) *Lehrbuch der Anthropologie in Systematischer Darstellung* (in German) Gustav Fischer Verlag, Stuttgart
- Nickerson BA, Fitzhorn PA, Koch SK, Charney M (1991) A methodology for near-optimal computational superimposition of two dimensional digital facial photographs and three-dimensional cranial surface meshes. *J Foren Sci* 36(2):480–500
- Park HK, Chung JW, Kho HS (2006) Use of hand-held laser scanning in the assessment of craniometry. *J Foren Sci Int* 160:200–206
- Pesce Delfino V, Colonna M, Vacca E, Potente F, Introna F (1986) Computer-aided skull/face superimposition. *Amer J Foren Med Pathol* 7(3):201–212
- Pétrowski A (1996) A clearing procedure as a niching method for genetic algorithms. In: *Proceedings of IEEE international conference on evolutionary computation*, pp 798–803
- Powell M (1964) An efficient method for finding the minimum of a function of several variables without calculating derivatives. *Comput J* 7:155–162
- Santamaría J, Córdón O, Damas S, Alemán I, Botella M (2007a) Evolutionary approaches for automatic 3D modeling of skulls in forensic identification. Applications of evolutionary computing. In: Giacobini M et al (eds) *Lecture notes in computer science*, vol 4448. Springer, Berlin, pp 415–422
- Santamaría J, Córdón O, Damas S, Alemán I, Botella M (2007b) A scatter search-based technique for pair-wise 3D range image registration in forensic anthropology. *Soft Comput* 11(9):819–828
- Santamaría J, Córdón O, Damas S, García-Torres JM, Quirin A (2009a) Performance evaluation of memetic approaches in 3D reconstruction of forensic objects. *Soft Comput* 13(8–9):883–904
- Santamaría J, Córdón O, Damas S, Ibáñez O (2009b) Tackling the coplanarity problem in 3D camera calibration by means of fuzzy landmarks: a performance study in forensic craniofacial superimposition. *IEEE Int Conf Comp Vis* 926:1686–1693
- Santamaría J, Córdón O, Damas S (2010) A comparative study of state-of-the-art evolutionary image registration methods for 3D modeling. *Comp Vis Image Underst* 115(9):1340–1354
- Seta S, Yoshino M (1993) A combined apparatus for photographic and video superimposition. In: Iscan MY, Helmer R (eds) *Forensic analysis of the skull*. Wiley, New York, pp 161–169
- Silva L, Bellon O, Boyer K (2005) Robust range image registration using genetic algorithms and the surface interpenetration measure. In: *Series in machine perception and artificial intelligence*. World Scientific Publishing Co. Pte. Ltd., Singapore
- Solis FJ, Wets RJB (1981) Minimization by random search techniques. In: *Informs (ed) Mathematics of operations research*, vol 6, USA, pp 19–30
- Stephan CN (2009) Craniofacial identification: techniques of facial approximation and craniofacial superimposition. In: Blau S, Ubelaker DH (eds) *Handbook of forensic anthropology and archaeology*. Left Coast Press, California, pp 304–321
- Stephan CN, Simpson E (2008a) Facial soft tissue depths in craniofacial identification—part I: an analytical review of the published adult data. *J Foren Sci* 53(6):1257–1272
- Stephan CN, Simpson E (2008b) Facial soft tissue depths in craniofacial identification—part I: an analytical review of the published sub-adult data. *J Foren Sci* 53(6):1273–1279
- Storn R (1997) Differential evolution—a simple and efficient heuristic for global optimization over continuous spaces. *J Global Optim* 11:341–359
- Taylor J, Brown K (1998) Superimposition techniques. In: Clement J, Ranson D (eds) *Craniofacial identification in forensic medicine*. Arnold, London, pp 151–164
- Ubelaker DH (2000) A history of Smithsonian-FBI collaboration in forensic anthropology, especially in regard to facial imagery. *Foren Sci Commun* 2(4)
- Ubelaker DH, Bubniak E, O'Donnell G (1992) Computer-assisted photographic superimposition. *J Foren Sci* 37(3):750–762
- Yamany SM, Ahmed MN, Farag AA (1999) A new genetic-based technique for matching 3D curves and surfaces. *Pattern Recognit* 32:1817–1820

- Yao J, Goh KL (2006) A refined algorithm for multisensor image registration based on pixel migration. *IEEE Trans Image Process* 15(7):1839–1847
- Yoshino M, Imaizumi K, Miyasaka S, Seta S (1995) Evaluation of anatomical consistency in craniofacial superimposition images. *Foren Sci Int* 74:125–134
- Yoshizawa S, Belyaev A, Seidel HP (2005) Fast and robust detection of crest lines on meshes. In: *SPM'05: proceedings of the 2005 ACM symposium on solid and physical modeling*. ACM Press, New York, pp 227–232
- Zadeh LA (1965) Fuzzy sets. *Inf Control* 8:338–353
- Zhang Z (1994) Iterative point matching for registration of free-form curves and surfaces. *Int J Comput Vis* 13(2):119–152
- Žitová B, Flusser J (2003) Image registration methods: a survey. *Image Vis Comput* 21:977–1000